Journal of Applied and Natural Science
16(4), 1690 - 1701 (2024)
ISSN : 0974-9411 (Print), 2231-5209 (Online)
journals.ansfoundation.org

Research Article

Neotectonic appraisal of Ramganga River basin, Eastern Kumaun, Himalaya, India

M. Nazish Khan
Department of Geography and Natural Resources, Samarkand State University, Samarkand, Uzbekistan
M. Suhail
Centre of Applied Remote Sensing and GIS Applications, Samarkand State University, Samarkand, Uzbekistan
Dilawez, Ali
Department of Geology, D.S. Degree College, Aligarh, India
S Mohd Wasi Haider Jafri
Aligarh Muslim University, India
Jamshid Jurayev
Department of Geography and Natural Resources, Samarkand State University, Samarkand, Uzbekistan

*Corresponding author. E-mail: nazishgeo@gmail.com

Article Info
https://doi.org/10.31018/jans.v16i4.5928
Received: July 4, 2024
Revised: November 27, 2024
Accepted: December 1, 2024

How to Cite
Khan, M. N. *et al.* (2024). Neotectonic appraisal of Ramganga River basin, Eastern Kumaun, Himalaya, India. *Journal of Applied and Natural Science*, 16(4), 1690 - 1701. https://doi.org/10.31018/jans.v16i4.5928

Abstract
The Ramganga River flows from north to south and drains the northeastern (Lesser Himalaya) of the Himalaya. It transects with numerous active faults, thrusts, and litho-tectonic units before the confluence with the Saryu River at Rameshwar.The present study aimed to determine the virtue of geomorphic indices in appraising the status of neotectonic activity in the Ramganga River Valley, Eastern Kumaun, Himalaya. The watersheds and drainage network were extracted using the Advanced Space-borne Thermal Emission and Reflection Radiometer (ASTER) DEM at 50000 and 100 Pixels threshold, derived18 sub-watersheds and detailed drainage network. Further, this study deciphered the relative neo-tectonic activity of the Ramganga river using the Index of Relative Active Tectonics (IRAT) based on various geomorphic indices Bifurcation Ratio (Br), channel sinuosity (Cs), Asymmetry Factor (Af), Hypsometric Integral (HI), Basin Elongation Ratio (Re), Drainage Density (Dd), Drainage Texture (Dt), and Stream Length Gradient (SL). These indices were classified into high, moderate and low to provide a rank to sub-basin for deriving the IRAT. The northeastern bank of Ramganga River shows high neo-tectonic activity, viz., stream length gradient (500- 1688), channel sinuosity (1.41- 1.48), and valley floor width to height ratio (0.11- 0.34) than southwestern parts.

Keywords: Digital Elevation Model, Faults and Thrusts, Index of Relative Active Tectonics (IRAT), Morphotectonic Indices, Ramganga

INTRODUCTION

The Himalayan orogeny is credited with causing the mountain range to arise due to a continental-continental collision between the Indian and Eurasian Plates approximately 65 million years ago in the Eocene period. (Valdiya, 1980; Dewey and Bird, 1970; McKenzie and Sclater, 1971; Molnar and Tapponnier, 1975; Farooq *et al.*, 2015; Kalpana *et al.*, 2023). This collision resulted in three north dipping major thrust zones viz., Main Central Thrust (MCT), Main Boundary Thrust (MCT), and Himalayan Frontal Thrust (HFT), displays youngness from north to south respectively (Valdiya, 1992). These thrusts are connected mainly by a range of tectonic structures and geomorphic features that are carried southward by collision and convergence (Kalpana *et al.*, 2023; Khan and Govil, 2023). In addition, the Himalaya exhibits a constant evolution in the form of active faults and thrusts, which are mirrored in the rising peaks, faults scarps, v-shaped canyons, shutter ridges, offset streams (including the 8848-meter-high Mount Everest) and magnificently varied landscape

(Beaumont *et al.*, 2001; Kothyari and Luirei, 2016; Kothyari *et al.*, 2019; Khan and Govil, 2023).

The lesser Himalayan system is divided into two classes in Kumaun, the lesser Himalaya viz., Inner Lesser Himalaya and Outer Lesser Himalaya system (Valdiya, 1980; Pant *et al.*, 2012; Farooq *et al.*, 2015; Kalpana *et al.*, 2023). Further, North Almora Thrust is considered as a separating unit between inner and outer Lesser Himalaya (Ahmad *et al.*, 2000; DeCelles *et al.*, 2001; Richards *et al.*, 2005; Kothyari *et al.*, 2017; Khan & Govil, 2023). The tectonic activity lies in the faults, and thrusts play a significant role in the geomorphic evolution of the drainage basins across the Himalayas. The youthfulness of the Himalayan terrain makes it ideal for studying basin morphometry and neo-tectonics which is reflected in the temporal landscape of research (Harrison *et al.*, 1997; Tapponnier *et al.*, 2001; Beaumont *et al.*, 2001; Farooq *et al.*, 2015; Kothyari and Luirei, 2016; Pant and Singh, 2017; Kothyari *et al.*, 2017b; Kothyari *et al.*, 2019; Kothyari *et al.*, 2020; Khan and Govil, 2023). Morphotectonic indices are a useful tool for assessing active tectonics. The impact of the interplay between tectonics, surface geological processes, climate change, rock resistance, and rock structures shapes the landscapes' evolution, as demonstrated by these indices. Rāmgangā river basin was selected for the current active tectonic evaluation which transects with numerous known/ unknown faults thrusts and lineaments from north to south viz., Vaikrita Thrust (VT), Munisiari Thrust (MT), Berinag Thrust (BT), Ramgarh Thrust (RT), Chiplakot and North Almora Thurst (NAT) (Farooq *et al.*, 2015). The present study was aimed to decipher neotectonic status and was carried out based on morphometric and morphotectonic indices including Drainage Density (Dd), Drainage Texture (Dt), Mean Stream Length Ratio (Sl), Bifurcation Ratio (Br), Drainage Basin Asymmetry (Af), Hypsometric Integral (HI), Channel Sinuosity (Cs), and Valley Floor Width and Height Ratio (Vf) through remote sensing and GIS which plays a pivotal role in providing spatial information needed for reckoning of these indices.

MATERIALS AND METHODS

Study area

The Ramganga River spans 1360 square kilometers and rises from the 3600-meter-high Namik Glacier. It lies between the Kali River on the Eastern side and the Sutlej River in the western side and shares its boundary with Goriganga River and Pindari River. The Main Boundary Thrust borders the Lesser Himalayan zone, which includes the Ramganga Basin, to the north, and the Main Central Thrust, which is the collective name for the wide fault zone dividing the Lesser Himalayan Sequence and Greater Himalayan Complex, borders it to the south. The Ramganga River spans approximately 78.6 km in a north-south direction. The basin is 26.5 km wide at its widest point and is located between latitudes 29°31'23" and 30°14'11"N and longitudes 80°06'12" and 80°06'49" E. The Ramganga receives numerous east and west small and large tributaries before joining the Saryu River at Rameshwar, near Ghat, in Pithoragarh. Large-scale landform features that resemble elongated valleys and ridges with remarkable parallelism characterize the region. Some notable geomorphic features include longitudinal ridges, valleys, knickpoints, offset streams, shutter ridges, and mountain fronts. One of the first signs of faulting and shearing in the region is thought to be the sub-parallel orientation of linear ridges and valleys. Narrow, extended valleys result from the softer, broken, and sheared rock eroding faster. The terrain has also been impacted by the differential erosion of different rock types juxtaposed due to fault movement. The meta-sedimentaries, or phyllites, schists, micaceous quartzites, amphibolites, and granitic gneisses, are exposed in and around the Ramganga basin trend in a WNW-ESE direction. On both banks are terraces made of sediments the river had deposited (Fig. 1).

Data and methods

The morphotectonic analysis of the Ramganga River was completed utilizing satellite data in conjunction with field research. The Digital Elevation Model (DEM) was produced using the Advanced Space-borne Thermal Emission and Reflection Radiometer (ASTER) data. It was also used to derive watersheds and the drainage network. The Japanese Ministry of Economy, Trade, and Industry (METI) constructed the ASTER instrument, which NASA's Terra spacecraft launched in December 1999. It uses three distinct telescopes and sensor systems to obtain satellite images across 14 spectral bands. Six shortwave infrared bands (SWIR) with a spatial resolution of 30 m, five thermal infrared bands (TIR) with a spatial resolution of 90 m, and three visible and near-infrared bands (VNIR) with a spatial resolution of 15 meters are among them. Each ASTER scene occupies a 60x60 km ground area. Further, Band 3 of VNIR acquired an along-track stereo coverage by a backward-looking telescope for producing a high-quality digital elevation model.

These 1:2500000 scale topographic maps were obtained from Army Map Services, which publishes them on behalf of the University of Texas at Austin, the organization in charge of publishing and distributing them. The WGS84 datum and UTM projection were used to georeference the downloaded maps (https://maps.lib.utexas.edu/maps/ams/). Using these georeferenced maps, the locations of towns, cities, and villages in the Ramganga river basin were vectorized.

A significant portion of the lithology, larger tectonic features such as thrusts and dislocations, and smaller

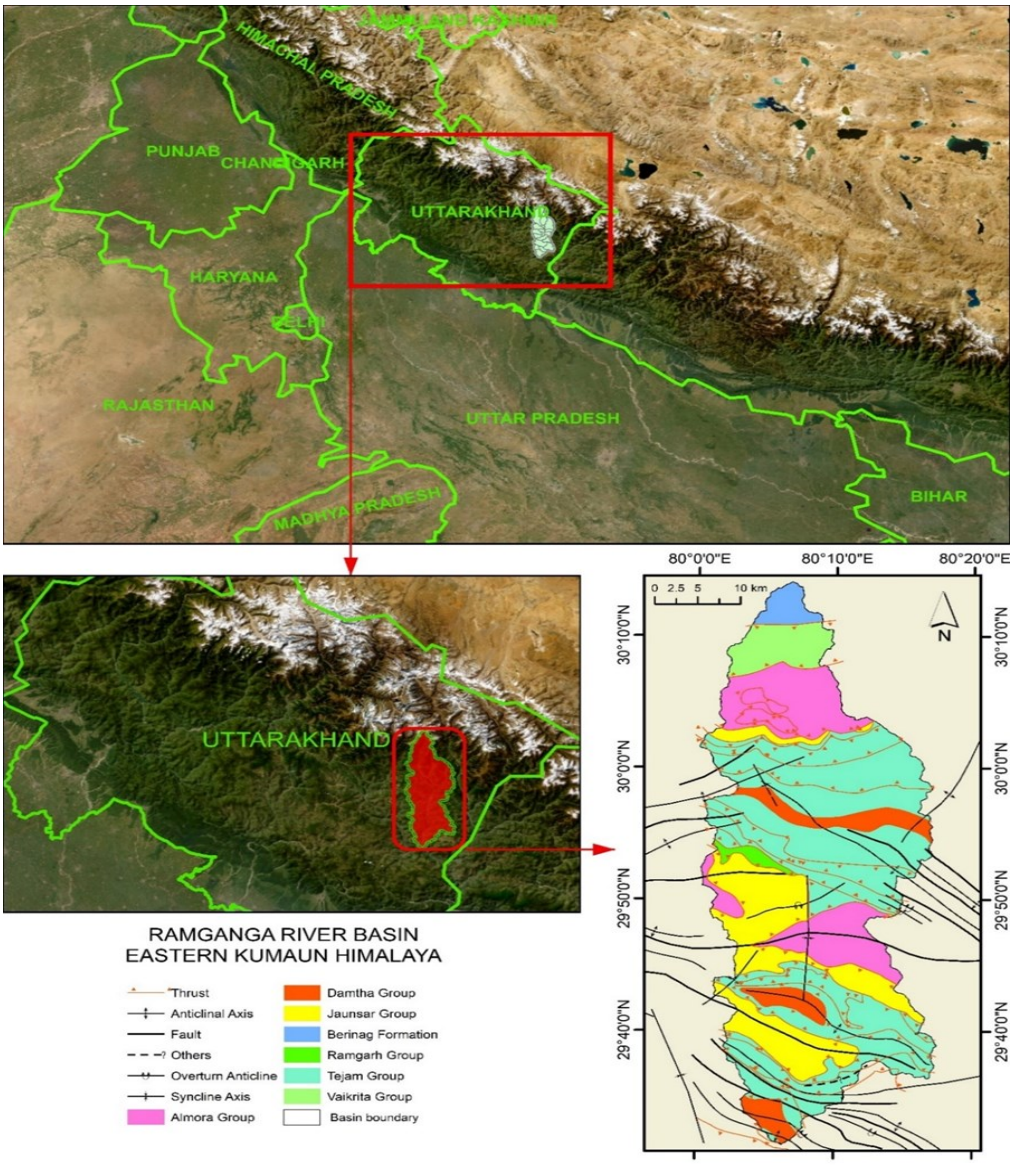

Fig. 1. *Showing the study area, geological, and structural map of Ramganga*

faults, joints, and shear zones are derived from the updated Valdiya (2010) geological map of the Kumaon Himalaya. The map was georeferenced to the WGS84 datum and UTM projection to be consistent with the ASTER DEM and multispectral data used in this work. Geological data was also gathered using published geological maps of the Kumaon Himalaya that could be georeferenced because they had a geographic referencing coordinate system (Fig. 1).

The TauDEM (Terrain Analysis Using Digital Elevation Models) plugin generated the stream networks and basin boundaries, and it also used the study area's digital elevation data to formulate various hydrologic characteristics. To define the borders, these hydrologic grids were incorporated into the GIS domain and used to locate all sites within the DEM upstream of the designated outlet point (Farooq *et al.*, 2015; Khan *et al.*, 2023; Khan and Govil, 2023).

Stream length gradient

The gradient of a stream's length can reveal how much soil and rock are being eroded in a river basin, transforming the surrounding terrain (Hack, 1973). In neotectonically active terrain, the erosion rate determines the uplift rate, which results in a slightly concave longitudinal profile (Schumm *et al.*, 2002), leading to crustal stability. However, tectonic, lithological, and climatic variables impact the stability of the terrain. Stream length gradient is defined as -

$$SL = \Delta H/\Delta L \qquad \text{Eq.1}$$

Where ΔH is the change in the elevation for a selected reach, and ΔL is the length of the reach and L is the total planimetric length from the midpoint of the reach to the highest point on the channel (Mahmood and Gloaguen, 2012). For current study, the stream length gradient was computed for 18 sub-basins of the Ram-

ganga river basin (Table 1).

Relief ratio

The relief (Rr) is the ratio of total basin relief (Difference in elevation at the summit and outlet of the basin) and basin length, measured as the longest dimension of the drainage basin (Schumm, 1956). It indicates the overall slope of the basin. It is defined as-

$$Rr = \frac{\Delta H}{L} \quad \text{Eq. 2}$$

Where ΔH is the relief of the basin and L is the length of the basin, measured in the longest dimension. Generally, the relief ratio decreases with the increase in the basin area. High relief ratio values reflect the potential for erosion and high tectonic activity, while low values correspond to moderate and low tectonic activity (Table 1).

Mean stream length ratio

The mean stream length ratio was calculated after deriving the stream length ratio of different orders of streams in the basin. Further, the mean stream length ratio was calculated using the following formula:

$$Lsm = Lu/nu \quad \text{Eq.3}$$

Where Lu is the mean length of all streams of one order and nu is the total number of streams of lower order. The means stream length ratio reflects a consistent relationship between the evolution of drainage and surface characteristics. This relationship can be explained in the form of tectonic activity (Table 1).

Channel sinuosity

Channel sinuosity is considered a sensitive marker to the active tectonics in the mountainous region. Generally, rivers rarely travel in a straight line due to the different forces exerted upon them, including tectonic and erosive forces. In addition, Straight river courses show values close to 1, while sinuous rivers show values beyond 1. It is a dimensionless parameter, calculated by dividing the length of the stream segment by the valley length. It is calculated by the following equation.

$$Cs = Sl/Vl \quad \text{Eq.4}$$

Where, Sl is the stream length calculated between two points and Vl is the valley length, it is the straight line length between two selected points. The channel sinuosity was calculated for 18 sub-basins (Table 1).

Drainage density

Drainage density is a significant morphometric index, the ratio of the total stream length of all orders in a basin to the basin area (Horton, 1932). It provides the numerical basis to understand the different components of basin evolution and describes the drainage fabric to understand the density of stream channels. A low drainage density occurs in permeable, highly vegetated, and slightly elevated regions while a high drainage density corresponds to rugged and highly elevated regions. Furthermore, the drainage density of a basin is influenced by the geologic and climatic conditions and is calculated using the equation.

$$Dd = Lu/A \quad \text{Eq.5}$$

Where Lu is the length of streams of all orders in a basin and A is the area of the basin (Table 1).

Drainage texture

The ratio of the total number of stream segments across all orders to the basin's perimeter is defined as the drainage texture (Horton, 1945). It was recognized that the infiltration capacity of the basin directly influences the drainage texture and it depends upon several natural factors such as climate, rainfall, vegetation, rock and soil type, relief, and evolution of the basin (Smith, 1950). The equation was used to calculate it.

$$T = \frac{Nu}{P} \quad \text{Eq. 6}$$

The drainage texture is denoted by T, the basin perimeter is represented by P, and Nu is the total number of stream segments across all orders (Table 01).

Drainage Frequency:

Drainage frequency, which is determined by dividing the total number of streams of all orders by the basin's area, is a significant morphometric indicator (Horton, 1932). The equation was used to calculate it.

$$Fs = \frac{Nu}{A} \quad \text{Eq.7}$$

where the area of the basin is denoted by A and the total number of stream segments across all orders is represented by Nu. According to Vijith and Sateesh (2006), permeability, infiltration capacity, and relief are the factors that determine the drainage frequency (Table 01).

Hypsometric integral

The hypsometric integral (HI) is the dimensionless parameter and provides a scale-free comparison of different watersheds or catchments. In addition, low values indicate eroded landscapes (late stage), moderate values indicate mature landscapes while high values correspond to young landscapes. The formula was used to calculate the hypsometric integral.

$$HI = \frac{Elmean - Elmin}{(Elmax - Elmin)} \quad \text{Eq.8}$$

Elmin is the basin's minimum elevation, Elmax is its maximum elevation, and Elmean is the basin's mean elevation (Table 01). The values of HI range between o

Table 1. Showing the morphotectonic parameters and their method of calculation with references

Aspects	Morphometric Indices	Formula	Reference
Linear	Channel Sinuosity (Cs)	Cs = Sl/Vl where Sl is stream length and Vl is valley length	Muller, 1968
	Drainage Density (Dd)	Dd = Lu/ A where Lu is the length of the stream of all orders and A is the area of the basin.	Horton, 1932
	Drainage Texture (Dt)	Dt = Nu/ P where Nu is the total number of streams and P is the perimeter of the basin.	Horton, 1932
	Drainage Frequency (Df)	Df = Nu/ A where Nu is the total number of streams and A is area of the basin	Horton, 1932
Aerial	Hypsometric Integral (HI)	HI = (ELmean- ELmin) / (ELmax- ELmin)where ELmean is the mean elevation, ELmin is the minimum, and ELmax the maximum elevation	Strahler, 1952
	Bifurcation Ratio (Br)	Br = Lu/ Lu+1 where Lu is the number of specified streams and a number of next higher-order streams in basin.	Strahler, 1964
	Asymmetry Factor (AF)	AF= Ar/ A where Ar is the area of right side of the basin and A is the total area of basin.	Cox *et al.*, 1994
	Valley Floor Width to Height Ratio (Vf)	Vf= 2Vfw/ (Eld-Esc) + (Erd-Esc), where Vfw= width of valley floor, Eld and Erd= Elevation of left and right valley divides, Esc= Elevation of the valley floor	Bull and McFadden, 1977
Relief	Stream Length Gradient Index (SL)	SL = Δh /ΔI×L, where Δh = Difference in elevation of the ends of the reach, ΔI = Length of reach, L = distance from the midpoint of reach to the most distant point up-stream.	Hack, 1973
	Relief Ratio (Rr)	Rb = H/L where H is the total relief of the basin and L is the length of the basin.	Schumn, 1956

and 1. Due to a lack of technological advancement, calculations in the past were difficult due to high processing and calculation costs. However, with the development of digital elevation models, it became a simpler and more accurate way to detect active tectonics Dowling *et al.*, 1998; Khan and Govil, 2023).

Bifurcation ratio

The number of streams of a given order divided by the number of streams of the next higher order is known as Rb (Schumm, 1956). Horton (1945) asserts that the bifurcation ratio is an index that characterizes a basin's relief and dissection. A narrow range of variation is observed for varying environmental conditions, except in areas where geology predominates. The following equation was used to calculate it.

$$Rb = \frac{\sum nu}{\sum Nu+1th\ order} \quad \text{Eq. 9}$$

Where Nu is the total number of streams of given order and Nu+1 is the total number of streams of the next higher order. Lower values of Rb correspond to the rolling and low elevation watershed while high values demonstrate the strong tectonic control over the evolution of basin. It was also observed by Eze & Effong (2010) that high values indicate a low risk of flash floods within the basin (Table 1).

Asymmetry factor

The asymmetry factor (AF) is an important morphotectonic parameter to trace tectonic tilting of a drainage basin (Cox *et al.*, 1994; Keller and Pinter, 2002; El Hamdouni *et al.*, 2008). It is based on that a river flowing in a homogeneous lithological terrain, which is not much affected by erosional and tectonic activities, is assumed to be a symmetric river. The AF is defined as-

$$AF = 100(\frac{Ar}{At}) \quad \text{Eq.10}$$

Where Ar is the right-side area of the basin from the trunk stream (headwater to outlet) and At is the total area of the basin (Table 1).

Valley floor width to height ratio

Bull and McFadden (1977) calculated the valley floor width-to-height ratio as an indicator of active tectonics to distinguish between open and broad-floored valleys. Tectonically active regions show considerably high variation in valleys in the form of v-shaped and U-shaped with a dynamic equilibrium. Silva *et al.* (2003) explored the distinctions between broad-floored, U-shaped valleys with primarily lateral erosion into nearby hills in response to tectonic quiescence and V-shaped valleys occupied by streams incising their bedrocks in response to active uplift. The Vf index was calculated using the equation (Table 1).

$$Vf = \frac{2Vfw}{(Eld-Esc)+(Erd-Esc)} \quad \text{Eq.11}$$

Vf is the valley floor width ratio to the height, Vfw is the valley width, Eld is the left divide's elevation, Esc is the valley floor's elevation, and Erd is the right divide's elevation (Fig. 4d).

Index of relative active tectonic activity:
The neo-tectonic activity was ascertained by evaluating the geomorphic indices. Further, these indices were classified into three categories: low tectonic activity, moderate tectonic activity, and high tectonic activity. These categories were combined to prepare an Index of Relative Active Tectonic Activity (IRAT). For this purpose, basins were classified by giving them a rank based on individual geomorphic index viz., if a basin has a low tectonic activity for Hypsometric Integral, was provided rank 1 while for moderate and high tectonic activity 2 and 3 ranks, respectively. Further, these ranks were averaged to provide a final tectonic rank for a basin.

RESULTS AND DISCUSSION

The morphotectonic indices were grouped into three sections for deriving results: relief, linear, and aerial parameters.

Stream order
The Ramganga river basin has a 1360 km^2 area with 5 orders of streams characterized by the dendritic, sub-dendritic parallel streams pattern (Fig. 2a). Due to significant tectonic influence, the trunk stream has a north-to-south trend, high sinuosity, and river displacement in many locations. The first and second-order streams, aligned parallel to the trunk streams of the sub-basin, showed an NNW and NNS trend, while the sub-basin streams were nearly aligned parallel to the trunk stream of the Ramganga River. Furthermore, many streams followed faults and thrust lines, indicating tectonic origin and also displayed meandering at many places.

Stream length gradient
The Stream Length Gradient (SL) calculated at multiple points in a sub-basin and average out the values for producing representative values. The SL values ranged between 36 and 1688 (Fig. 2b). The results of stream-line gradient indicated that the northwest portion of the basin exhibits significant tectonic influence, whereas the sub-basins that crossed the trunk stream showed correspondingly low tectonic activity (Bashir *et al.*, 2023). However, low values also corresponded to the tectonic activity due to transecting faults and thrusts across the basin (Fig. 2b).

Relief ratio
The results of Rr showed remarkable variation and ranged from 0.14 to 1.04 for 18 sub-basins. The highest values of RR observed in the Central Eastern sub-basins. A high relief ratio corresponds to ruggedness and steep topography while low values indicate plain and U-shaped valleys (Gautam *et al.*, 2020). In addition, the Ramganga exhibited moderate to high tectonic activity in its northern, central, and eastern regions, whereas its southwestern region displays low tectonic activity (Fig. 2c).

Mean stream length ratio
The results of the mean stream length ratio ranged from 0.18 to 0.43. In addition, these were divided into three classes to represent how the drainage basin's evolution was influenced by active tectonics and erosion (Anand and Pradhan, 2019). It suggests that the mean stream length ratio reflects a close proximity to faults and thrusts, transecting with the Ramganga river basin. The central and southeastern parts showed high values, while the East-Central part showed correspondingly low values (Fig. 2d).

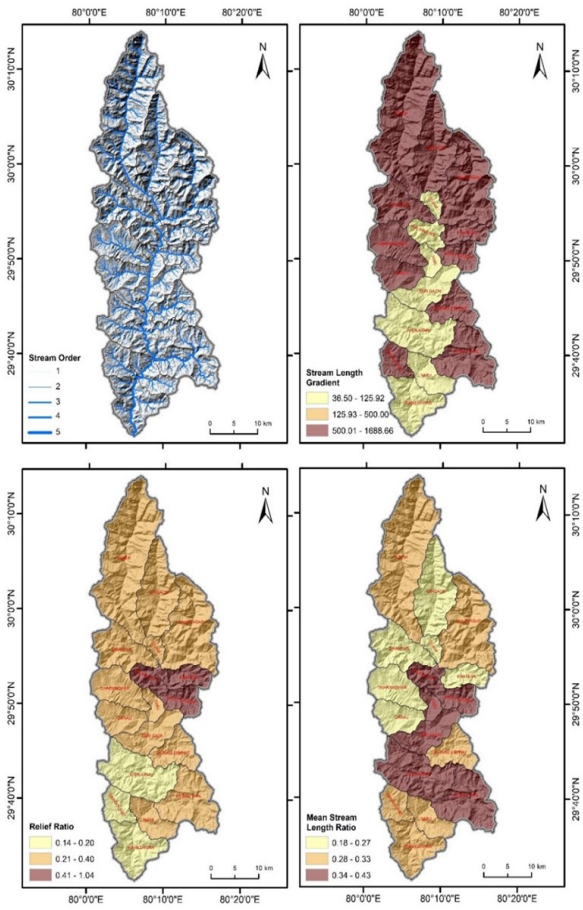

Fig. 2. *Displays stream order, stream length gradient, relief ratio, & mean stream length ratio of the Ramganga River Basin*

Channel sinuosity

It is an indicator to measure the youthfulness of the topography. In the present study, the Channel Sinuosity was calculated at multiple points to prepare a representative value for each sub-basin to produce precise and accurate results. The channel sinuosity values range between 1.01 and 1.48, exhibiting straight to sinuous streams. Ramganga river basin transects with numerous known and unknown faults and thrusts like Munisiari Thrust, and Main Central Thrust, resulting in parallel streams, meandering, and high sinuosity. Further, these curved, parallel, and meandering streams could be attributed to tectonic influence rather than mature topography. Results were observed for 18 sub-basins of Ramganga River Basin, indicative of strong tectonic uplift in Bansbagad, Jaurasi Didihat, and Kholasan sub-basins while southeastern sub-basins exhibit moderate neotectonic activity.

Drainage density

The drainage density for each of the 18 sub-basins was computed and classified into three classes to determine the spatial distribution and provide a rank for each sub-basin. The drainage density displays a remarkable variation from 1.31 to 5.68. The Khatera sub-basin, located in the central-eastern periphery, had a very high drainage density, while the northern and southern regions had a low drainage density. Numerous faults and thrusts were noted to cross the Ramganga river basin (Fig. 1). The region was significantly impacted by tectonic activity, a primary cause of erosion and uplift, revealing the results (Gautam *et al.*, 2020). The central western region had a correspondingly high drainage density, indicating relatively more tectonics than erosion, whereas the northern and south-central regions showed low drainage density (Fig. 3b).

Drainage texture

The calculated drainage texture values for 18 sub-basins varied between 1.38- 7.26. The drainage texture values are divided into three classes to provide a rank to each sub-basin. The high values were indicative of impermeability, low infiltration, and high relief, while low values correspond to permeable lithology, high infiltration, and moderate relief (Farooq *et al.*, 2015; Bahrami and 2023). The fine texture was observed in the Namik (Northern extremity) and Khatera (Central-Eastern border), while other northern and southern sub-basins display comparatively moderate texture. Central sub-basins demonstrate low drainage texture (Fig. 3c).

Drainage frequency:

The results of drainage frequency were derived for 18 sub-basins and further categorized into three classes. The drainage frequency values range from 3.08 to 4.54, indicative of tectonic and erosive forces controlling the basin evolution in the Ramganga River Basin. Further, high values corresponded to relatively high relief and lower infiltration capacity (Fig. 3d). Low values were indicative of high erosion and low active uplift (Bahrami and Martin, 2023). The sub-basins (Tejam, Thal, and Naini) exhibited high values and more streams per square kilometers. These sub-basins were located close to the trunk stream. It was observed that strong tectonic activity had strong control over the evolution of the drainage network.

Hypsometric integral (HI)

According to El Hamdouni *et al.* (2008) and Khan and Govil (2023), the hypsometric integral is a crucial morphometric indicator for estimating the basin volume that has not been eroded. The high values are indicative of youthful topography while low values indicate denuded and eroded landscape. Ramganga river basin originates in the Lesser Kumaon Himalaya with a maximum of 6800 meters and 500 meters' minimum elevation, indicating a high gradient with a variety of landscapes. To decipher the neotectonic status of the Ramganga river basin, the HI values have been computed for 18 sub-basins, ranging from 0.27 to 0.58. Furthermore, these values have been grouped into three tectonic classes viz., 0.27- 0.31, 0.31- 45 and <0.45. HI values over the basin show a mosaic of strong tectonic influence from east to west and from north to south. The trunk stream crosses the Tejam and Thal sub-basins, resulting in low values because of high erosion and low uplift. At the central western extremity, the Dharmgarh and Darau sub-basin show a prominent control of tectonic activity, imitated by high values. Furthermore, the High values in the Ramganga River indicate strong tectonic control as it approaches the basin's southern region (Fig. 4a).

Bifurcation ratio

The overall bifurcation ratio results categorized into three classes for providing a rank to each sub-basin, based on low, moderate, and high values (Gautam *et al.*, 2020). The results vary widely in the Ramganga river basin, with values ranging from 0.45 to 5.0. Furthermore, results were analyzed in combination with existing known and unknown faults and thrusts (Fig. 01) to demonstrate the neotectonic ranking. It observed that the Ramganga river basin exhibited strong tectonic influence in the southern region while upper catchment of the basin shows the control of deforming processes. Importantly, the strong elevation gradient created a substantial path for water to flow, and most sub-basins from north to south (Namik to Thal) had low bifurcation ratio values, which caused more erosion. However, it was also noted that more erosion occurred when different tectonic features struck with each other.

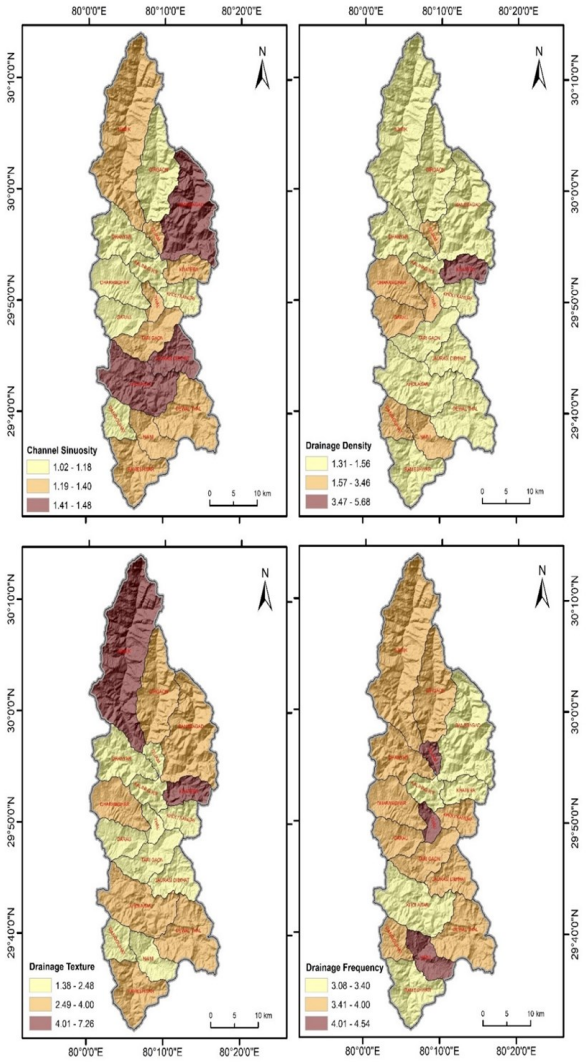

Fig. 3. *Showing channel sinuosity, drainage density, drainage texture and drainage frequency*

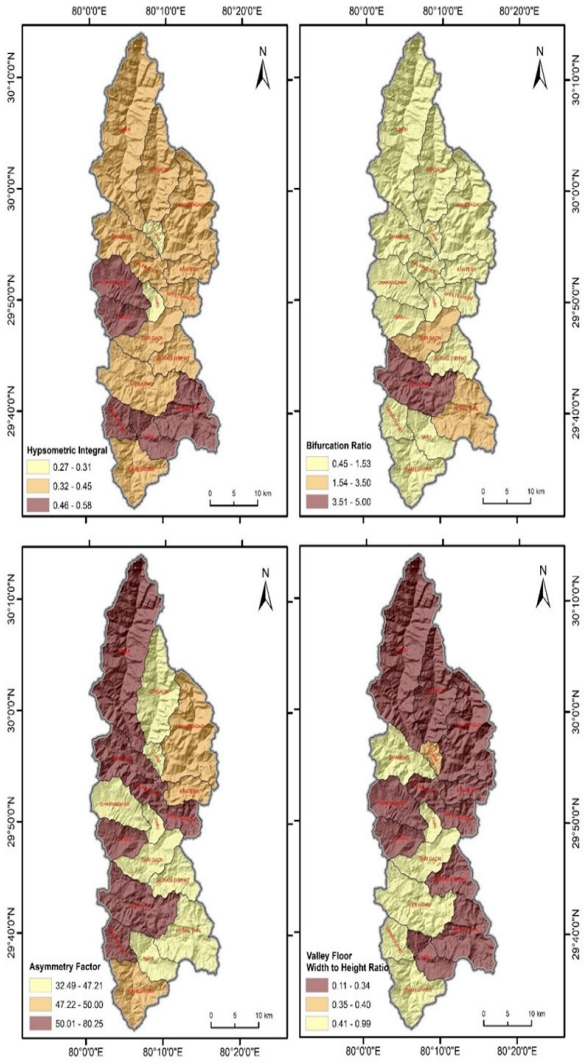

Fig. 4. *Showing hypsometric integral, bifurcation ratio, asymmetry factor, valley floor width to height ratio*

Asymmetry factor (AF)

The values of AF for the 18 sub-basins of Ramganga River ranged between 32.49 and 80.25 (Fig. 04a). Based on tilting, the values were classified into three classes to derive the tectonic importance of a sub-basin. Sub-basins that fall into the nearly symmetric category were given a low rank, and those that fall into the highly asymmetric category were given a high rank. Basin tilting and asymmetry increased in tectonically active regions where basins were affected by increased erosional activity. Regional scale tectonic activity is indicated by the tilting and migration of higher-order streams in active river basins, while an increase in sub-basin asymmetry indicates localized tectonic activity (Keller and Pinter, 2002; Ahmed *et al.*, 2020). The Ramganga river basin exhibits high asymmetry on both banks and anonymously low asymmetry on the north-eastern and extreme south basins. Low values are seen in the Central and Southeast sub-basins, which indicates that the trunk stream was pushed to the right by tectonic action. The lowest rank was assigned to Rameshwar, Khatera, and Bansbagad sub-basins due to their closeness to symmetry.

Valley floor width and height ratio (Vf)

The Ramganag River is a north-south draining river and confluence with the Saryu river. During its travel from Namik glacier to Tejam, it runs through different lithological and structural domains. These litho-structural domains directly influence the transformation of river from high-rise v-shaped valleys to moderately uplifted U-shaped valleys. The results of the valley floor width-to-height ratio suggest that the Ramganga river basin is highly dominated by structural control while the sub-basins transect with the main stream reflect more domination of erosive forces. The values of Vf ranged

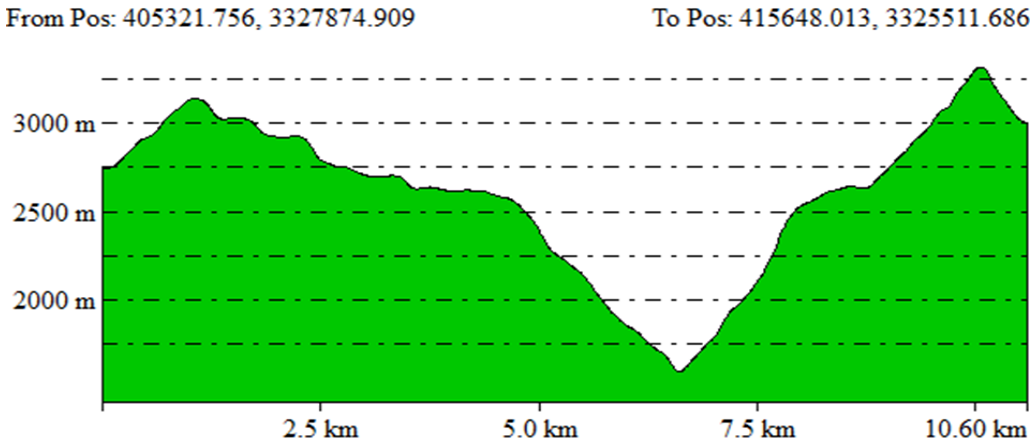

Fig. 5. *Method of calculating valley floor width to height ratio*

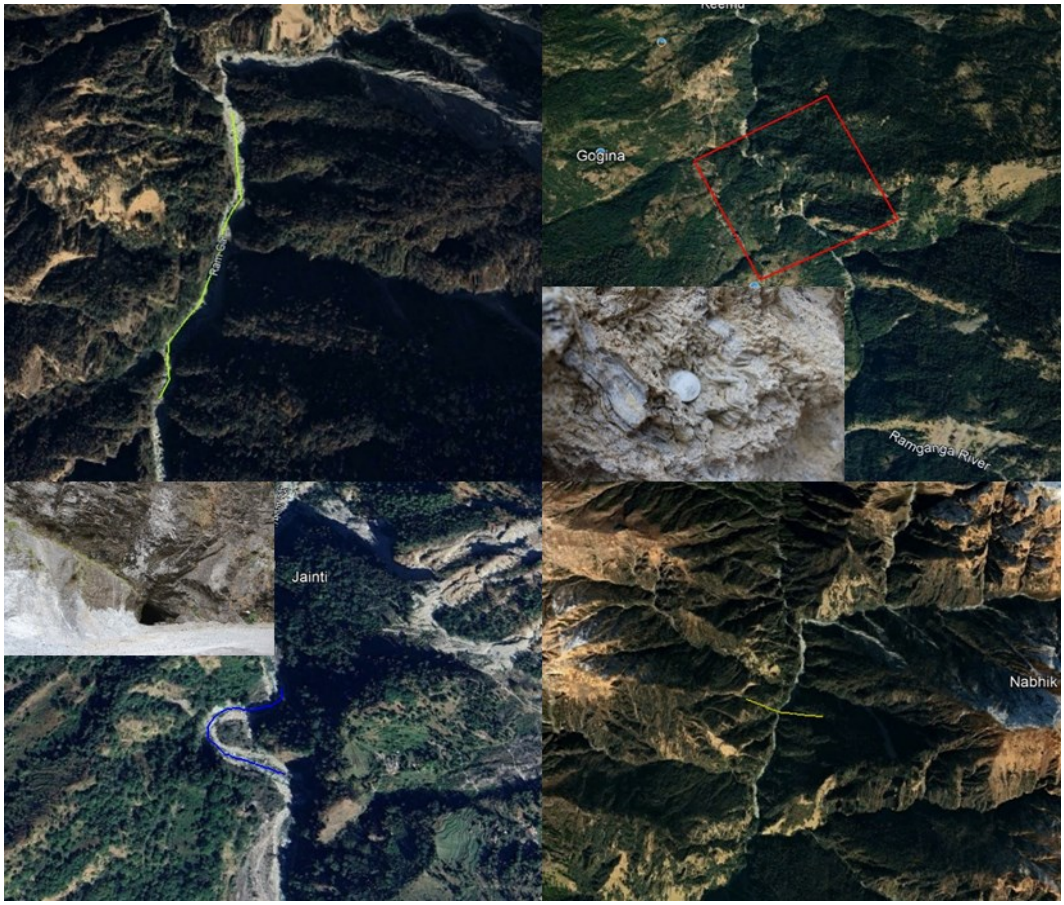

Fig. 6. *Showing the different field tectonic evidences, collected during field work*

between o.11 and 0.99. These results clearly revealed a consistent and strong encounter between erosive and tectonic forces (Anusree *et al.*, 2024). The sub-basins aligned perpendicular to the trunk stream showed correspondingly strong control of tectonics, while the trunk stream carved sub-basins differently, resulting in rapid erosion and low uplift.

Field and other evidence of active tectonics

Field observations were made to collect evidence of tectonic influence along the Ramganga River. Further, it was backed up with satellite imageries (Google Earth Pro) to delineate a few instances of tectonic control over the Ramganga River. The Ramganga River cut across many known and unknown faults and thrusts. Satellite-based evidence like straightward river course and abrupt changes in the flow direction indicate strong tectonic control. During field visits, imprints of active tectonics collected in the form of fault gouges and breccias, hydrothermally altered mineral assemblages indicating faulted zones, landslides, unpaired river terraces, ponding of rivers, paleochannels, paleolake deposits, uplifted potholes, deep gorges with convex walls, and stream offsets at selected locations (Fig. 6). Tec-

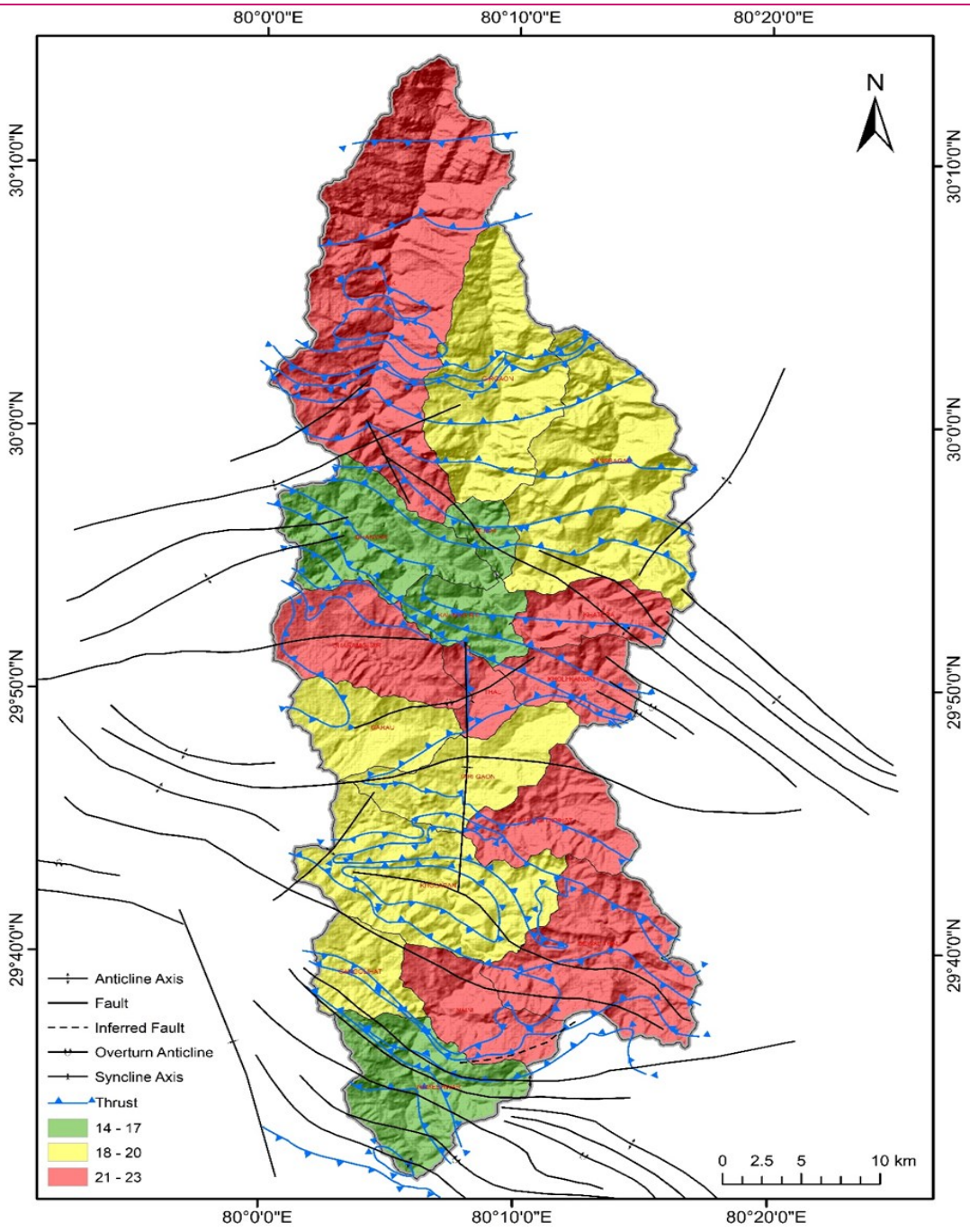

Fig. 7. *Showing the final tectonic map of Ramganga based on IRAT, clearly depicts variability of neotectonic activity along different faults and thrusts*

tonically derived landforms produced a change in morphometry of the basin.

Index of relative active tectonics

A single index alone as a measure of active tectonics is likely to produce a vague and conflicting assessment. A more accurate assessment of a region's tectonic status is more likely to result from the application of multiple index combinations (Dowling *et al.*, 1998; Ali and Iqbal, 2020). This study evaluated active tectonics in a relatively moderate area (1360 km2), demarcated into 18 sub-basins using 11 morphotectonic indices to make a reliable and accurate assessment. In order to achieve this, 18 sub-basins were ranked according to the values of each indicator, which ranged from 1-3. A basin should receive a score of 33 if it experiences the highest level of tectonic activity and a score of 11 if it experiences the least amount of tectonic activity. Eight of the 18 sub-basins of the Ramganga belonged to strong tectonic activity, six sub-basins displayed moderate tectonic active tectonics, while four sub-basins exhibited low tectonic activity. The sub-basins exposed strong tectonic activity and were not transecting with the trunk stream except Thal sub-basin. It indicated that

the tectonic features dominated the structural evolution of sub-basins if they did not lie close to the mainstream. Sub-basins are located close to Ramganga and exhibit moderate to low tectonic activity, indicative of stronger erosive forces than tectonics (Fig. 7).

Conclusion

Based on morphotectonic parameters, the Ramganga river basin exposed strong neotectonic control, and erosive forces played a significant role in the basin evolution. Imprints of active tectonics and erosional processes were clearly seen in the Ramganga River basin, including abrupt changes in river courses, fault aligned linear streams and valleys, parallel tributaries, and tilted sub-basins. The tectonic activity aligned to thrusts and faults coupled with a strong stream length gradient turn into strong erosive force along with the trunk stream. However, Namik sub-basin is located in the northern extremity and transects with Main Central Thrust (MCT), resulting in strong tectonic influence. It carved broad floored valleys due to glacial movement, most of them perpendicular to the river's main course. Further, tectonic forces had the strength to determine the path of Ramganga River and modify the course at many places. It was also observed that the morphotectonic parameters are significant in displaying the degree and direction of tectonic modifications in the Ramganga river basin with remote sensing and GIS.

Conflict of interest

The authors declare that they have no conflict of interest.

REFERENCES

1. Ahmad, T., Harris, N., Bickel, M., Chapman, H., Bunbury, J. & Prince, C. (2000). Isotopic constraints on the structural relationships between the Lesser Himalayan Series and the High Himalayan Crystalline Series, Garhwal Himalaya. *Geol. Soc. Amer. Bull*., 112, 467–477. https://doi.org/10.1130/0016-7606(2000)112%3C467:ICOTSR%3E2.0.CO;2
2. Ahmed, F. & Rao, K. S. (2016). Hypsometric analysis of the Tuirini drainage basin: a geographic information system approach. *Journal of the Indian Society of Remote Sensing*, 44 (2), 273–280.
3. Ali, S.A. & Ikbal, J., (2020). Assessment of relative active tectonics in parts of Aravalli mountain range, India: implication of geomorphic indices, remote sensing, and GIS. *Arab J Geosci* **13**, 57. https://doi.org/10.1007/s12517-019-5028-2
4. Anand, A.K. & Pradhan, S.P. (2019). Assessment of active tectonics from geomorphic indices and morphometric parameters in part of Ganga basin. *J. Mt. Sci*. 16, 1943–1961. https://doi.org/10.1007/s11629-018-5172-2
5. Anusree, K. K. Ajayakumar, A. Reghunath, R. & Santhosh, V. (2024). Morphometric and morphotectonic characteristics of a Tropical River Basin, North Kerala, India using geospatial technology. *International Journal of River Basin Management*, 1–20. https://doi.org/10.1080/15715124.2024.2400690
6. Bashir, B. Abdullah A. Hussein, B. & Mahmoud, E. (2023). GIS Analysis for Active Tectonics Assessment of Wadi Al-Arish, Egypt. *Applied Sciences* 13, no. 4: 2659. https://doi.org/10.3390/app13042659
7. Beaumont, C. R.A. Jamieson, M.H. Nguyen, & Lee B. (2001). Himalayan tectonics explained by extrusion of a low-viscosity crustal channel coupled to focused surface denudation, *Nature,* 414, 738-742. https://doi.org/10.1038/414738a
8. Bahrami, S. & Stokes, M. (2023). Analyzing drainage basin orientation and its relationship to active fold growth (Handun anticline, Zagros, Iran), *Geomorphology*, V- 426. https://doi.org/10.1016/j.geomorph.2023.108605.
9. Bull, W. & L.D. McFadden, (1977). Tectonic Geomorphology North and South of the Garlock fault. California, *Journal of Geomorphology*, 1, 15-32.
10. Cox, R. T. (1994). Analysis of drainage basin symmetry as a rapid technique to identify areas of possible Quaternary tilt-block tectonics: An example from the Mississippi Embayment. *Geological Society of America Bulletin,* 106(5), 571–581. https://doi.org/10.1130/0016-7606(1994)106%3C0571:AODBSA%3E2.3.CO;2
11. DeCelles, P.G. Robinson, D.M. Quade, J. Ojha, T.P. Garizone, C.N. Copeland, P. & Upreti, B.N. (2001). Stratigraphy, structure, and tectonic evolution of the Himalayan fold-thrust belt in western Nepal. *Tectonics*, 20, 487–509. https://doi.org/10.1029/2000TC001226
12. Dewey, J.F. & Bird, J.M. (1970). Mountain Belts and the New Global Tectonics. *J. Geophys. Res*. 75 2625-2647. https://doi.org/10.1029/JB075i014p02625
13. Dowling, T.I. Richardson, D.P. O'Sullivan, A. Summerell, G.K. & Walker, J. (1998). Applications of the hypsometric integral and other terrain based metrices as indicators of catchment health: A preliminary analysis. CSIRO Land and Water, (Canberra). *Technical Report* 20/98, 49.
14. El Hamdouni, R. Irigaray, C. Fernández T. Chacón, J. & Keller, E.A. (2008). Assessment of relative active tectonics, southwest border of the Sierra Nevada (southern Spain), *Geomorphology,* 96, 150–173. https://doi.org/10.1016/j.geomorph.2007.08.004
15. Eze, B.E. & Effiong, J. (2010). Morphometric Parameters of the Calabar River Basin: Implication for Hydrologic Processes. *Journal of Geography and Geology*, 2, 18-26. https://doi.org/10.5539/jgg.v2n1p18
16. Farooq, S. Khan, M.N. & Sharma, I. (2015). Assessment of Active Tectonics in Eastern Kumaon Himalaya on the Basis of Morphometric Parameters of Goriganga River Basin. *IJAEES*, 3(3), 14-21.
17. Gautam, P.K. Singh, D.S. Kumar, D. Singh, A.K. (2020). A GIS-based Approach in Drainage Morphometric Analysis of Sai River Basin, Uttar Pradesh, India. *Journal of Geological Society of India,* 95, 366–376. https://doi.org/10.1007/s12594-020-1445-9
18. Hack, J.T. (1973). Stream-profile analysis and stream-gradient index. *United States Geological Survey Journal of Research*, 1(4), 421–429.
19. Harrison, T. M. Grove, M. Lovera, O. M. & Catlos, E. J. (1998). A model for the origin of Himalayan anatexis and

inverted metamorphism. *Journal of Geophysical Research*, 103, 27017–27032. https://doi.org/10.1029/98JB02468
20. Harrison, T. M. Ryerson, F. J. LeFort, P. Yin, A. Lovera, O. & Catlos, E. J. (1997). A late Miocene-Pliocene origin for the Central Himalayan inverted metamorphism, *Earth Planet. Sci. Letter*, 146, E1-E7. DOI:10.1016/S0012-821X (96)00215-4.
21. Horton, R.E. (1932). Drainage Basin Characteristics. *Trans. Am. Geophys*. Union, 13, 350-361.
22. Horton, R.E. (1945). Erosional Development of Streams and their Drainage Basins: Hydrophysical Approach to Quantitative Morphology. *Geol. Soc. Am. Bull.,* 56: 275-370.
23. Kalpana. G. Kothyari, G.C. & Kotlia, B.S. (2023). Morphotectonic assessment of the Gaula river basin, Kumaun lesser Himalaya, Uttarakhand. *Quaternary Science Advances*, 12, 100- 115. https://doi.org/10.1016/j.qsa.2023.100115.
24. Keller, E.A. & Pinter, N. (2002). Active Tectonics: Earthquakes, Uplift and Landforms (2nd Edition). *Prentice Hall, New Jersey*, 362. ISBN: 0130882305.
25. Khan M.N. & Govil H. (2023). Assessment of On-going tectonic deformation in the Goriganga River Basin, Eastern Kumaon Himalaya Using Geospatial Technology. *Journal of Applied and Natural Science*, 15(4), 1679 – 1690.
26. Khan, M. N. Khudoyarova, S. S. Juraev, J. & Mamajanov, R. (2023). Field-based Tectonic Assessment and Spatial Correlation with Land Use and Land Cover in the Goriganga River Basin. *Bulletin of Pure & Applied Sciences-Geology*, 42F (1), 32–45.
27. https://doi.org/10.48165/bpas.2023.42F.1.4.
28. Kothyari G.C. & Pant P.D. (2008). Evidence of active deformation in the Northwestern part of Almora in Kumaon Lesser Himalaya: A geomorphic perspective. *Jour. Geol. Soc. Ind.*, 72, 353-364.
29. Kothyari, G.C. Dumka, R.K. Singh, A.P. Chauhan, G. Thakkar, M.G. & Biswas, S.K. (2017). Tectonic evolution & stress pattern of South Wagad Fault at the Kachchh Rift Basin in western India. *Geological Magazine*. 154(4), 875-887. doi:10.1017/S0016756816000509.
30. Kothyari, G. C. Kandregula, R. S. & Luirei, K. (2017). Morphotectonic records of neotectonic activity in the vicinity of North Almora Thrust Zone Central Kumaun Himalaya. *Geomorphology*, 285, 272–286.
31. Kothyari, G.C. Kotlia, B.S. Talukdar, R. Pant, C.C. & Joshi, M. (2020). Evidences of neotectonic activity along Goriganga River, Higher Central Kumaun Himalaya, India. *Geological Journal*, 55 (9), 0072- 1050. https://doi.org/10.1002/gj.3791
32. Kothyari, G.C. Joshi, N. Taloor, A.K. Kandregula, R.S. Kotlia, B.S. Pant, C.C. & Singh, R.K. (2019). Landscape evolution and deduction of surface deformation in the Soan Dun, NW Himalaya, India. *Quaternary International*, 507, 302-323. https://doi.org/10.1016/j.quaint.2019.02.016.
33. Kothyari, G.C. & Luirei, K. (2016). Late Quaternary tectonic landforms and fluvial aggradation in the Saryu River valley: Central Kumaun Himalaya. *Geomorphology*, 268, 159-176. https://doi.org/10.1016/j.geomorph.2016.06.010.
34. Mahmood, S.A. & Gloaguen, R. (2012). Appraisal of active tectonics in Hindu Kush: Insights from DEM derived geomorphic indices and drainage analysis. *Geoscience Frontiers,* 3(4), 407-428. https://doi.org/10.1016/j.gsf.2011.12.002
35. McKenzie, D. & Sclater, J.G. (1971). The Evolution of the Indian Ocean since the Late Cretaceous". *Geophysical Journal International*, 24 (5), 437.
36. Molnar, P. & Tapponnier, P. (1975). Cenozoic tectonics of Asia: Effects of a continental collision. *Science,* 189, 419-426.
37. Muller, J. E. (1968). An introduction to the hydraulic and topographic sinuosity indexes. *Annals Association of American geographers,* 58, 371-385.
38. Pant, C.C. & Singh, S.P. (2017). Morphotectonic analysis of Kosi River basin in Kumaun Lesser Himalaya: an evidence of neotectonics. *Arab J Geosci*, 10, 421. https://doi.org/10.1007/s12517-017-3213-8.
39. Pant, P.D. Chauhan, R. & Bhakuni, S.S. (2012). Development of transverse fault along North Almora Thrust, Kumaun Lesser Himalaya, India: A study based on field and magnetic fabrics. *J Geol Soc India*, 79, 429–448. https://doi.org/10.1007/s12594-012-0068-1
40. Richards, A. Argles, T. Harris, N. Parrish, R. Ahmad, T. Darbyshire, F. & Draganits, E. (2005) Himalayan architecture constrained by isotopic tracers from clastic sediments: Earth Planet. *Sci. Lett.*, 236, 773–796.
41. Schumm, S.A. (1956). Evolution of Drainage Systems and Slopes in Badlands at Perth Amboy, New Jersey. *Geol. Soc. Am. Bull.,* 67, 597-646.
42. Silva, P.G. Goy, J.L. Zazo, C. & Bardajm, T. (2003). Fault-generated mountain fronts in southeast Spain: Geomorphologic assessment of tectonic and seismic activity. *Geomorphology*, 50(1-3), 203-225.
43. Strahler, A. N. (1952). Hypsometric (area-altitude) analysis of erosional topography. *Geological Society of America Bulletin*, 63(11), 1117–1142.
44. Strahler, A.N. (1964). Quantitative geomorphology of drainage basins and channel networks. In: V. T. Chow (ed), Handbook of Applied Hydrology. *Mc GrawHill Book Company*, New York, section 4-II.
45. Valdiya, K.S. (1992). Active Himalayan Frontal Fault Main Boundary Thrust and Ramgarh Thrust in Southern Kumaun. *Journal of Geological Society of India*, 40(6), 509–528.
46. Valdiya, K.S. (2010). The Making of India: Geodynamic Evolution. New Delhi, *Macmillan Publishers India Ltd*. 816. ISBN: 0230-32833-4.
47. Valdiya, K.S. (1980). Geology of the Kumaun Lesser Himalaya: Dehra Dun, India, Wadia Institute of Himalayan Geology, 291.
48. Vijith, H. & Satheesh, R. (2006). GIS based morphometric analysis of two major upland sub-watersheds of meenachil river in Kerala. *J Indian Soc Remote Sens.,* 34, 181–185. https://doi.org/10.1007/BF02991823